Evidence for Multiple Open and Inactivated States of the hKv1.5 Delayed Rectifier

Thomas C. Rich* and Dirk J. Snyders#
*Department of Biomedical Engineering and #Departments of Medicine and Pharmacology, School of Medicine, Vanderbilt University, Nashville, Tennessee 37232 USA

ABSTRACT The kinetic properties of hKv1.5, a *Shaker*-related cardiac delayed rectifier, expressed in *Ltk*$^-$ cells were studied. hKv1.5 currents elicited by membrane depolarizations exhibited a delay followed by biphasic activation. The biphasic activation remained after 5-s prepulses to membrane potentials between −80 and −30 mV; however, the relative amplitude of the slow component increased as the prepulse potential approached the threshold of channel activation, suggesting that the second component did not reflect activation from a hesitant state. The decay of tail currents at potentials between −80 and −30 mV was adequately described with a biexponential. The time course of deactivation slowed as the duration of the depolarizing pulse increased. This was due to a relative increase in the slowly decaying component, despite similar initial amplitudes reflecting a similar open probability after 50- and 500-ms prepulses. To further investigate transitions after the initial activated state, we examined the temperature dependence of inactivation. The time constants of slow inactivation displayed little temperature and voltage dependence, but the degree of the inactivation increased substantially with increased temperature. Recovery from inactivation proceeded with a biexponential time course, but long prepulses at depolarized potentials slowed the apparent rate of recovery from inactivation. These data strongly indicate that hKv1.5 has both multiple open states and multiple inactivated states.

INTRODUCTION

The *Shaker*-related hKv1.5 potassium channel has been cloned from human heart (Philipson et al., 1991; Tamkun et al., 1991), has an identified counterpart in human myocytes (Wang et al., 1993), and has been identified in human atrium and ventricle using histochemical techniques (Mays et al., 1995) and in atrium using antisense techniques (Feng et al., 1997). Both the voltage dependence of activation and the delayed rectifier phenotype of hKv1.5 indicate that it may be involved in the regulation of the plateau duration and the subsequent repolarization of the cardiac action potential (Wang et al., 1993; Snyders et al., 1993). In addition, the sensitivity of hKv1.5 currents to quinidine, clofilium, and other drugs suggests that it is a target for class III antiarrhythmic agents (Snyders et al., 1992; Malayev et al., 1995; Snyders and Yeola, 1995). This channel is also expressed in brain, visceral smooth muscle, and pancreatic β-cells (for review see Deal et al., 1996). Thus, detailed understanding of the kinetics of this channel is an important prerequisite to understanding its contribution in several physiological roles, including the cardiac action potential, and to understanding mechanisms underlying drug channel interactions.

Previous studies of hKv1.5 have indicated that, similar to *Shaker*, hKv1.5 displays a steep voltage dependence of activation, an apparent voltage dependence in the amount of inactivation, voltage-independent inactivation time constants, and biexponential deactivation (Zagotta and Aldrich, 1990; Hoshi et al., 1991, 1994; Snyders et al., 1993; Stefani et al., 1994; Bezanilla et al., 1994; Zagotta et al., 1994a,b). The purpose of this study was to further examine the relationships between open, closed, and inactivated states after initial channel opening. In contrast to *Shaker*, we did not observe a Cole-Moore shift (Cole and Moore, 1960). Both the biexponential activation kinetics and the dependency of the deactivation time course on the duration of the preceding depolarization suggest the presence of multiple open states.

MATERIALS AND METHODS

Cell preparation

In this study we used a stable mouse *Ltk*$^-$ cell line expressing hKv1.5 as previously described (Snyders et al., 1993). Cells were cultured in Dulbecco's modified Eagle's medium supplemented with 10% horse serum and 0.25 mg/ml G418. The cultures were passed every 4–5 days using a brief trypsin treatment. Before experimental use, cultures were incubated with 2 μmol/L dexamethasone for 12–24 h to induce efficient channel expression. The cells were removed from the dish with a rubber policeman, stored at room temperature, and used within 12 h.

Ltk$^-$ cells were used in this study because of the small levels of endogenous currents, as illustrated in Fig. 1. As noted previously (Snyders et al., 1993), the current-voltage relationship of blank or sham-transfected L-cells is linear up to approximately +40 mV. Positive to +40 mV, a small superimposed time-independent outward current was noted (typically <50 pA at +60 mV). Fig. 1 shows that even the largest endogenous currents displayed little or no time dependence and lacked detectable tail currents both at room temperature (23°C) and at elevated temperature (33°C in this example).

Received for publication 1 July 1997 and in final form 1 April 1998.

Address reprint requests to Dr. Dirk Snyders, VIB Department of Molecular Biophysics, Physiology and Pharmacology, University of Antwerp, UIA T4.22, Universiteitsplein 1, B-2610 Wilrijk, Belgium. Tel.: 32-3-820-2335; Fax: 32-3-820-2541; E-mail: dsnyders@uia.ua.ac.be.

0006-3495/98/07/183/13 $2.00

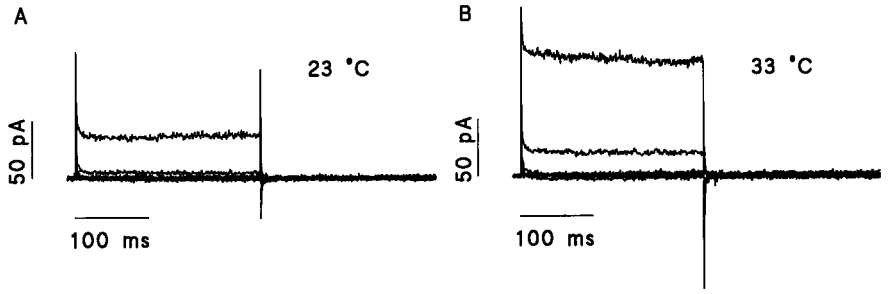

FIGURE 1 Endogenous current in the *Ltk*$^-$ cell line. Currents were elicited by steps to membrane potentials between −80 and +60 mV from a holding potential of −80 mV (in 10-mV steps). The tail currents were measured at −30 mV. The tracings represent one of the largest endogenous currents we observed in these control experiments; no compensation was used. (*A*) Currents at 23°C. An endogenous current is evident only at +50 and +60 mV. These currents displayed little or no time dependence, and even after strong depolarization no tail currents are observable. (*B*) Currents at 33°C. Although the endogenous current was larger at higher temperatures, it still exhibited little time dependence. No deactivating tail currents were observed.

Electrical recording

Recordings were made with an Axopatch-200 or 200A patch clamp amplifier (Axon Instruments, Foster City, CA) using whole-cell configuration. Pipettes were pulled from starbore borosilicate glass (Radnoti Co., Monrovia, CA) and heat polished. Bath temperature (20–45°C) was controlled using a Peltier device. Unless indicated otherwise, the holding potential was −80 mV. To ensure adequate voltage control (in the whole-cell configuration), the pipette resistance was limited to 3 MΩ and averaged 2.3 ± 0.1 MΩ (n = 43). Voltage offsets were zeroed with the pipette in the bath solution; no additional correction was made for the liquid junction potential difference, which, with the solutions used, is estimated to be <5 mV (Barry and Lynch, 1991; Neher, 1992). Pipettes were then lowered onto the cells and gigaohm seals were formed by applying light suction (10.2 ± 1.0 GΩ). After achieving whole-cell configuration, capacitive transients were elicited by applying both positive and negative 20-mV steps from the holding potential (−80 mV) and recorded at 40 kHz (filtered at 10 kHz) for calculation of access resistance and input impedance. Capacitance and series resistance compensation were then optimized to achieve 80% compensation. We calculated the residual resistance and excluded those experiments in which the voltage error due to series resistance exceeded 5 mV. Current records were sampled at 2–10 times the anti-alias filter setting and were acquired using a 16-bit resolution Analogic HSDAS16 A/D board (Analogic Corp., Wakefield, MA). Software for acquisition was designed in-house using Visual Basic and DriverLINX/VB drivers (Scientific Software Tools, Malvern, PA). This software allows for custom protocols (both stimulation and sampling) not available in commercial packages.

Solutions

The intracellular pipette filling solution contained (in mM) 110 KCl, 10 HEPES, 5 K_4BAPTA, 5 K_2ATP, and 1 $MgCl_2$ and was adjusted to a pH of 7.2 using KOH, giving a final K^+ concentration of ~145 mM. The standard bath solution contained (in mM) 130 NaCl, 4 KCl, 1.8 $CaCl_2$, 1 $MgCl_2$, 10 HEPES, and 10 glucose and was adjusted to a pH of 7.35 with NaOH. To obtain higher extracellular K^+ concentrations, equimolar substitution of KCl for NaCl was used. The pH of the solutions decreased ~0.1 units with a 10°C increase in temperature due to the temperature dependence of the buffer. Thus, the pH of the solutions at high temperature remained within 0.2 pH units of the pH at room temperature. Such small changes in pH did not significantly affect gating at room temperature.

Analysis

Data acquired in the whole-cell configuration were assessed by calculating time constants of activation, inactivation, and deactivation. A linear fit of the current-voltage relationship for currents elicited by voltage steps to potentials below the threshold of activation was extrapolated to correct for passive leak. All software for the analysis presented was written in-house using Visual Basic, FORTRAN, or MATLAB. Simulations assumed Markov models (i.e., the transition rates between states were not functions of time). The curve-fitting procedure to calculate time constants (and their relative amplitudes) used either a nonlinear least-squares (Gauss-Newton) algorithm or a simplex algorithm. The number of exponentials required and goodness of fit were evaluated by inspecting the residuals for nonrandom trends and comparing X^2 values statistically. Results are expressed as mean ± SEM with the number of observations, n, given in parentheses.

RESULTS

hKv1.5 currents elicited by depolarizations from a holding potential of −80 mV to potentials above 30 mV displayed biphasic activation (Fig. 2). After an initial delay, most of the activation time course could be described with a single fast component representing approximately 70% of the total amplitude in a biexponential fit. Nevertheless, a component of smaller amplitude was consistently observed (Fig. 2). We sought to determine whether the second component of activation occurred due to a hesitant closed state delaying the opening of a small population of channels or due to the equilibration between multiple open states.

A prepulse-independent second component of activation

To determine whether a hesitant closed state precedes channel activation we examined the prepulse dependence of the two components of activation. If a hesitant state exists, then the occupancy of this state should be reduced by depolarizing the channels to potentials near the threshold of channel opening before pulsing to strongly depolarized potentials. In other words, the long prepulses would promote the occupancy of closed states near the open state and reduce the occupancy of the hesitant state. Therefore, we recorded currents elicited by steps to +50 mV after 5-s prepulses to potentials between −70 mV and −10 mV. The currents elicited after conditioning steps to −40 mV or more negative potentials all superimposed (Fig. 3 *A*); thus, no Cole-

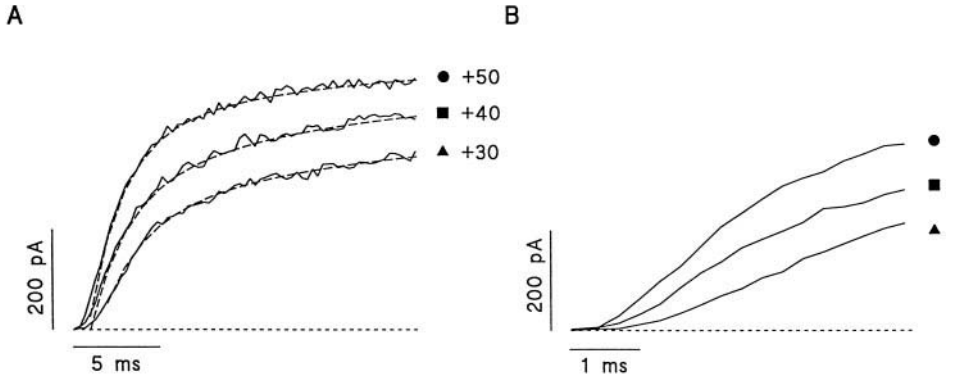

FIGURE 2 Kinetics of hKv1.5 activation. (*A*) Two components in the activation time course of hKv1.5 currents. Tracings are shown for step depolarizations to +30, 40, and 50 mV from a holding potential of −80 mV. Dashed lines represent double exponential fits of activation time course (time constants: τ_1 = 2.0, τ_2 = 11.3 ms, 78% $A_{\tau 1}$ at 30 mV; τ_1 = 2.0, τ_2 = 11.3 ms, 79% $A_{\tau 1}$ at 40 mV; τ_1 = 1.9, τ_2 = 10.4 ms, 88% $A_{\tau 1}$ at 50 mV). (*B*) An expanded view of the first 5 ms of the activation time course. The delay in activation indicates that multiple closed states exist before channel activation.

Moore shift (Cole and Moore, 1960) was observable. We found that after prepulse potentials between −70 mV and −30 mV both components of activation remained (Fig. 3 *A* and *C*). This was also the case with prepulses to −30, −25, and −20 mV, as shown in Fig. 3 *B* where current tracings were scaled such that the amplitudes of the time varying components are equal. This figure clearly shows that the first component was significantly reduced after the −20-mV prepulse but not after the −30- and −25-mV prepulses. Fig. 3 *D* shows that as the prepulse potential was raised above the threshold of hKv1.5 activation (≈−30 mV, dashed line represents the quasi-steady-state activation

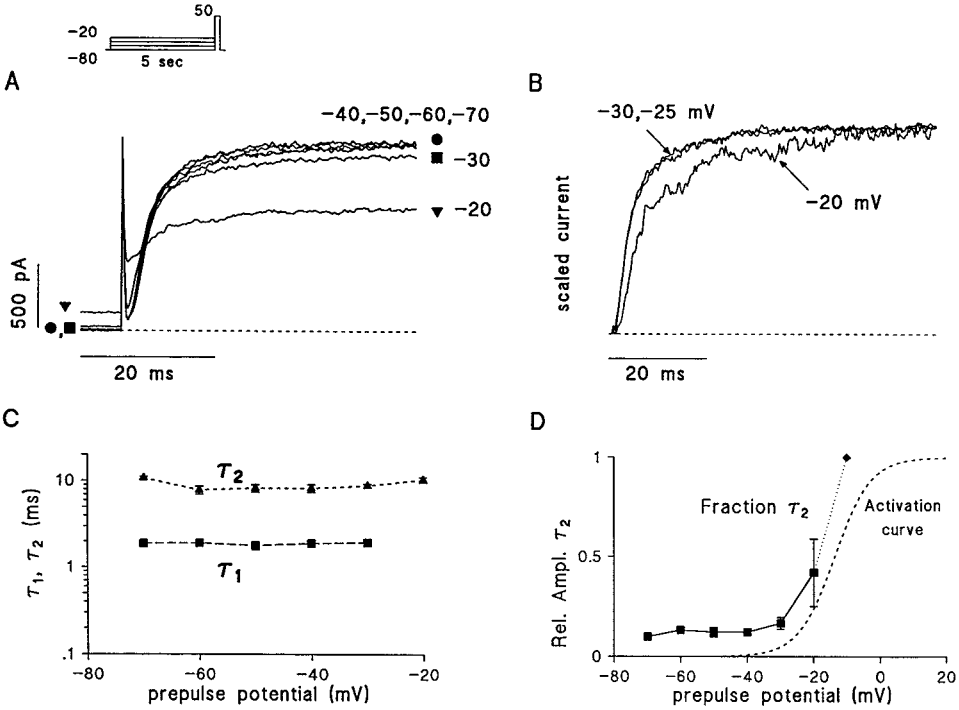

FIGURE 3 Dependence of hKv1.5 activation time course on prepulse potential. (*A*) hKv1.5 currents elicited after 5-s prepulse to membrane potentials between −60 and −20 mV (inset depicts pulse protocol). Symbols are added to identify the tracings (●, −60 to −40 mV; ■, −30 mV; ▲, −20 mV). No Cole-Moore shift is visible in this voltage range ($\tau_1 \approx 2$, $\tau_2 \approx 8$ ms, $A_{\tau 1} \approx 90\%$ between −60 and −40 mV; τ_1 = 2.3, τ_2 = 10 ms, $A_{\tau 1}$ = 87% at −30 mV; τ_1 = 2.3, τ_2 = 12.3 ms, $A_{\tau 1}$ = 70% at −20 mV). This figure is representative of five additional experiments. (*B*) Current traces from the same experiment as *A* scaled such that the time course of channel activation ranges from zero to 1. The scaled tracings show an apparent slowing of channel activation after the −20-mV prepulse but not after the −30- or −25-mV prepulses. (*C*) Time constants of activation as a function of prepulse potential. The fast component of activation was not consistently observable after prepulses to −20 mV. (*D*) Relative amplitude of the slow component of activation (■). The dashed line represents the Boltzmann equation fit to the quasi-steady-state activation curve obtained from tail current amplitudes after 500-ms depolarizations. Data are from four to six experiments (mean ± SEM). After the −10-mV prepulse, only a slow component was detectable when residual activation was observable (see text for details).

curve), the fast component of activation disappeared, but the slow component of activation remained. With prepulses to −20 mV (▲ in Fig. 3 *A*), the slow component was always observable, but the fast component was not consistently observable. Activation kinetics at +50 mV after a prepulse to −10 mV were more difficult to analyze as the majority of channels were already activated during this conditioning step. Despite this limitation, we observed only the slow exponential component of activation in the experiments in which the residual activation could be analyzed. The persistence of the slow component of activation in the available pool of channels suggested that this component was not due to slow recruitment from a hesitant closed state and that the biexponential time course could reflect equilibration between multiple open states.

The deactivation time course depends on the duration of activating pulse

Another indication of multiple open states would be a biexponential relaxation of ionic current at potentials below the threshold for channel opening (~−30 mV) after a strong depolarization (a fully activated protocol, Fig. 4). Multiexponential relaxation has been described previously for both *Shaker* (Zagotta et al., 1994b) and hKv1.5 (Snyders et al., 1993) K^+ channels but does not necessarily imply multiple open states (Correa and Bezanilla, 1994; Zagotta et al., 1994b). The biexponential tail current decay can be modeled with either multiple closed states or with multiple open states. However, one prediction of a multiple open state system is that the deactivation time course would depend on the duration of the activating pulse. To test whether the duration of the depolarizing pulse would influence the tail current time course, we recorded tail currents at membrane potentials between −60 and −30 mV after pulses to +50 mV of variable duration (see inset of Fig. 4 *B*). The order of prepulse duration was randomized in each experiment. We found that increasing the duration of the depolarizing pulse resulted in a slowing of the tail current decay (Fig. 4). The time course of channel deactivation could be described with a biexponential function regardless of the duration of the preceding depolarization. However, after short depolarizations, the time constants of the biexponential fits were considerably faster than those after long depolarizations; at a membrane potential of −50 mV the two tail current time constants slowed from $\tau_{5:1} = 11.5 \pm 1.4$ and $\tau_{5:2} = 46 \pm 1.0$ ms ($n = 5$) after a 5-ms step to +50 mV to $\tau_{50:1} = 24 \pm 2$ and $\tau_{50:2} = 80 \pm 10$ ms ($n = 5$) after a 50-ms step to +50 mV (where $\tau_{x:1}$ and $\tau_{x:2}$ indicate the two time constants for the fit to the data obtained after a prepulse of duration x, in milliseconds). The superposition of tail currents after 50-ms (●), 500-ms (■), and 5000-ms (▲) activating pulses consistently showed slower tail current decay after longer activating pulses (Fig. 5 *A–D*). Peak

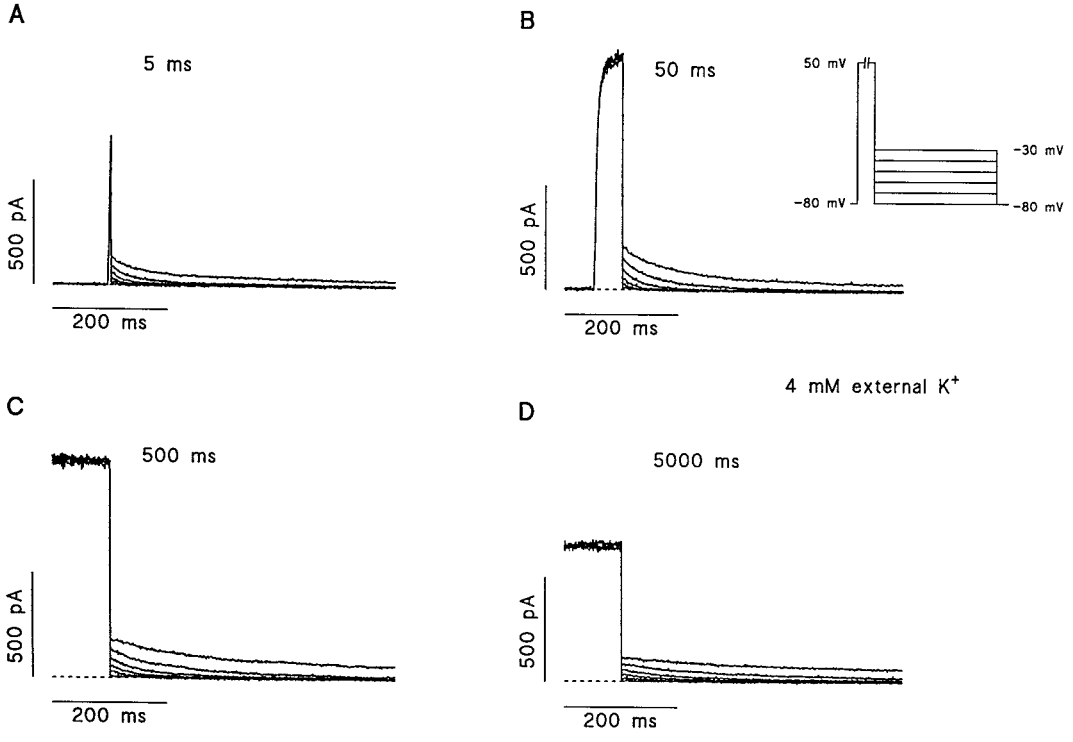

FIGURE 4 hKv1.5 currents after (*A*) 5-, (*B*) 50-, (*C*) 500-, and (*D*) 5000-ms pulses to +50 mV in 4 mM external K^+ (inset depicts pulse protocol). The amplitude of the current declined as the conditioning pulse duration was increased from 50 to 5000 ms, reflecting slow inactivation. However, the time course of deactivation was also modified with the apparent loss of the fast component of current decay after longer prepulses (compare *B* and *D*).

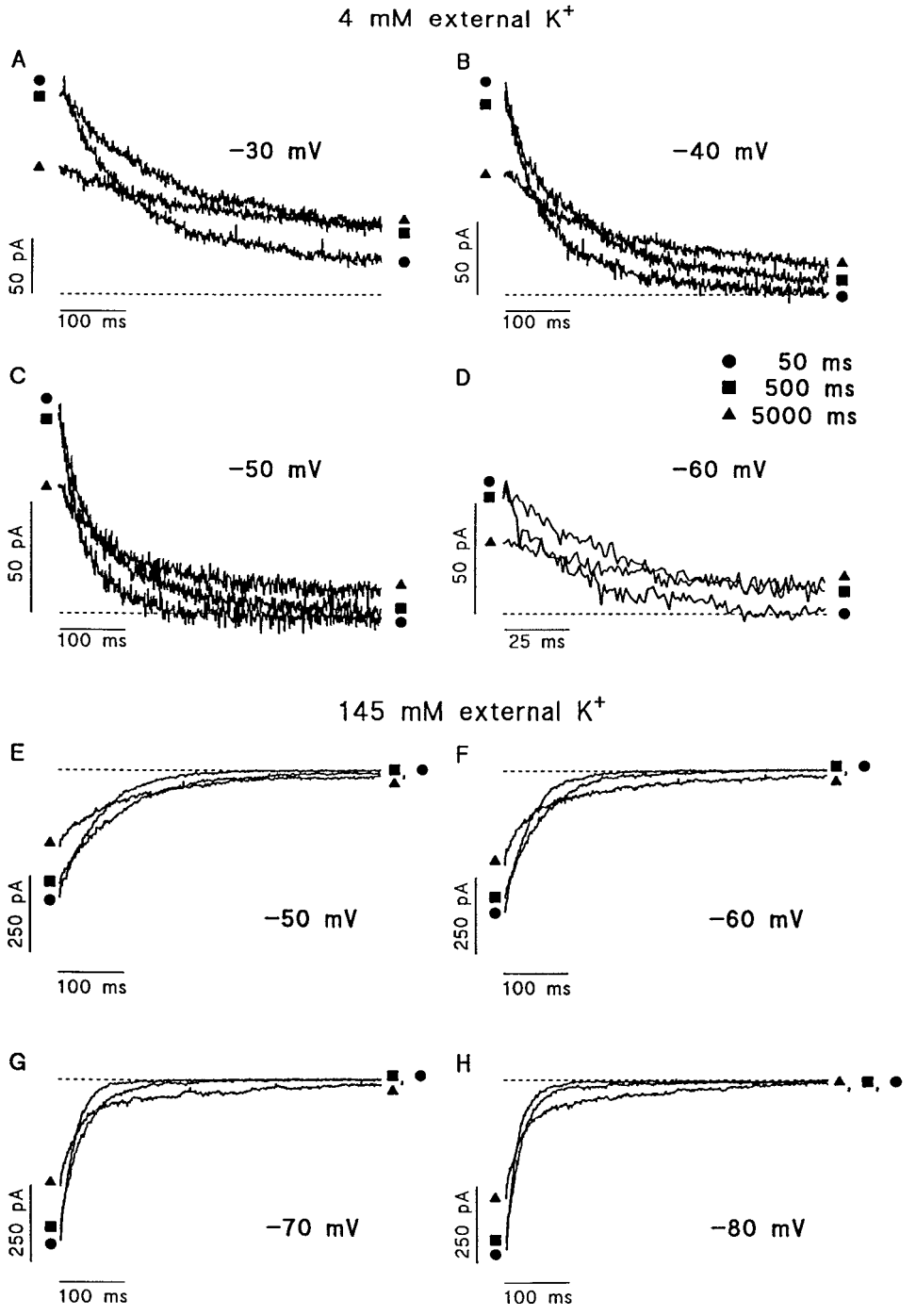

FIGURE 5 hKv1.5 tail currents after 50 (●), 500 (■), and 5000 ms (▲) at (*A*) −30 mV, (*B*) −40 mV, (*C*) −50 mV, and (*D*) −60 mV in 4 mM external K^+ and at (*E*) −50 mV, (*F*) −60 mV, (*G*) −70 mV, and (*H*) −80 mV in 145 mM external K^+. *A–D* represent expanded and superimposed views of the tails currents from Fig. 4. Despite similar initial amplitudes after 50- and 500-ms prepulses, the decay is considerably slower after the 500-ms prepulse. After the 5000-ms prepulse, the initial amplitude was lower (due to partial inactivation), but the additional slowing resulted in a crossover phenomena (crossover was observed at each voltage in each experiment ($n \geq 4$)).

tail currents after 500-ms activating pulses were 86 ± 4% of peak tail currents after 50-ms activating pulses, consistent with the reduction of current due to inactivation (after 500 ms, current levels at 50 mV were 85 ± 2% of those at 50 ms; $n = 8$).

To more closely examine the tail current decay at lower membrane potentials, we used high external K^+ (145 mM K^+) to increase the tail current amplitudes (Fig. 5 *E–H*). The time course of decay was faster at −80 mV ($\tau_{50:1}$ = 12 ± 2 and $\tau_{50:2}$ = 42 ± 8 ms; $n = 5$) than at −50 mV ($\tau_{50:1}$ = 31 ± 8 and $\tau_{50:2}$ = 75 ± 20 ms; $n = 5$). As in 4 mM external K^+, longer depolarizations to +50 mV resulted in tail currents that decayed with slower time constants. The superposition of deactivating tail currents after 50-, 500-, and 5000-ms depolarizations resulted in tail current crossover indicative of an increased contribution from the slower components. Regardless of the prepulse duration, the tail currents followed a biexponential time course (Fig. 6). The fastest exponential component ($\tau_{5:1}$ = 6.6 ± 0.9 ms at −80 mV; $n = 6$) was observable only after a 5-ms depolarization. This component was either slowed or was not observable after depolarizations of 50 ms ($\tau_{50:1}$ =

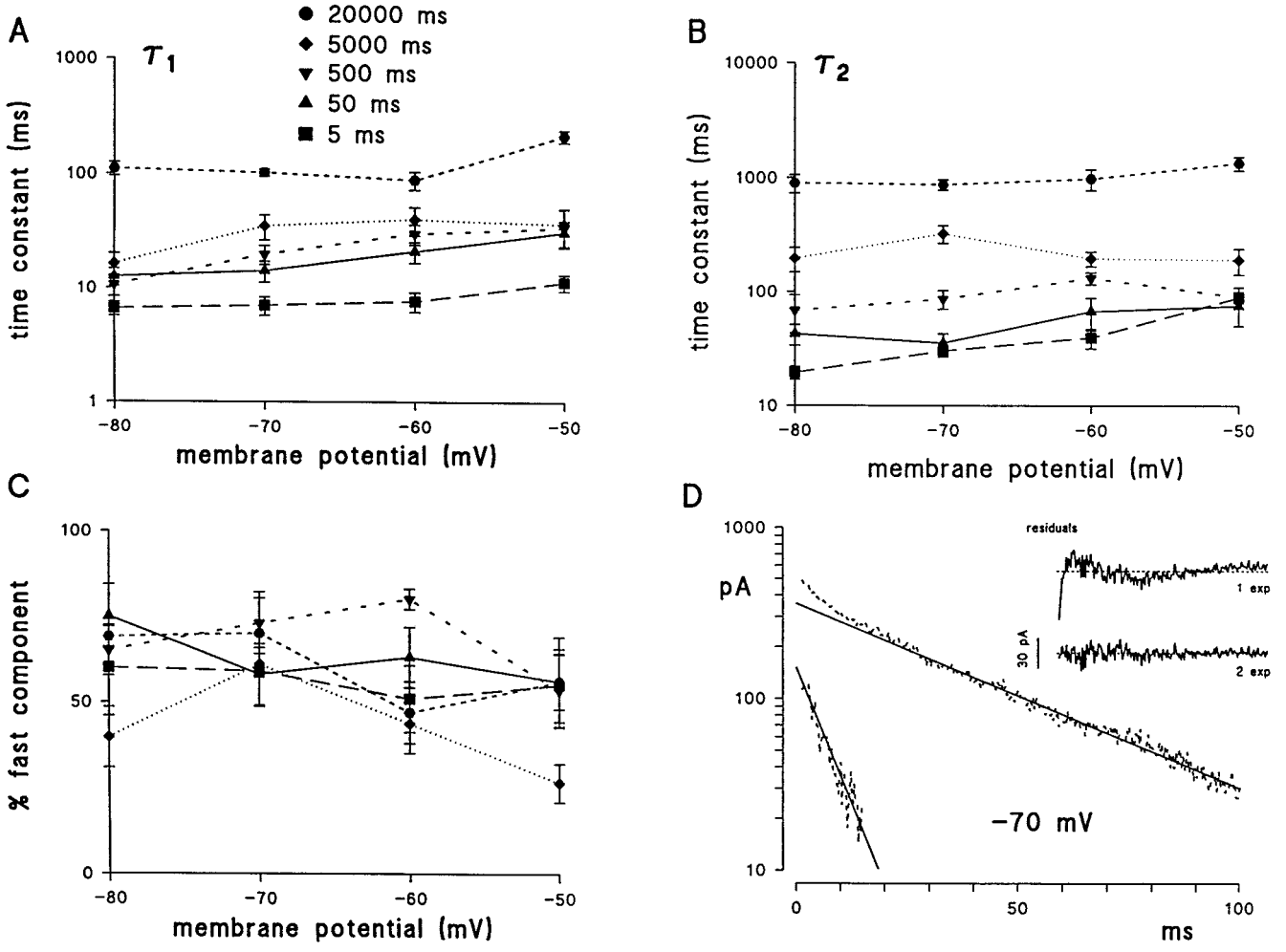

FIGURE 6 Kinetics of hKv1.5 tail currents in 145 mM external K^+ after depolarizations of different duration to +50 mV; durations are indicated by the symbols in the inset of *A*, which applies to *A–C*. (*A*) The fastest observable time constant for each condition. (*B*) The slower time constant observed for each condition. (*C*) Contribution to the total amplitude of the faster observed component. (*D*) A representative biexponential fit of tail current at −70 mV after a 5-ms depolarization to +50 mV. The inset shows the residual error for monoexponential and biexponential fits to the tail current time course (monoexponential: τ = 32.5 ms; biexponential: τ_f = 6.9 ms, τ_i = 40.5 ms, $A_{\tau 1}$ = 30%). The systematic deviations in the monoexponential fit were absent with the biexponential fit.

12.6 ± 2.2 ms at −80 mV; n = 7) and depolarizations of 5 s ($\tau_{5000:1}$ = 16.4 ± 3.8 ms at −80 mV; n = 4).

Multiple inactivated states

Previously, we reported that the apparent degree of hKv1.5 inactivation increased with elevated temperature (Snyders et al., 1993). We further examined the temperature dependence of inactivation to determine whether 1) the increase in the amplitude of inactivation occurred because the transitions into the inactivated states were temperature dependent or 2) the apparent temperature dependence of inactivation is due to preceding temperature-dependent transitions. Fig. 7 *A* is a representative tracing of hKv1.5 currents elicited by 5-s pulses to +50 mV at three temperatures. From the normalized current tracings it is apparent that significantly more inactivation occurred at higher temperatures (Fig. 7 *B*). In fact, at temperatures above 32°C three distinct exponential components (τ_1, τ_2, and τ_3) were observable in the time course of inactivation. Fig. 7 *C* shows the time constants for the time course of inactivation at 22°C (■), 28°C (▲), 32°C (♦), and 36°C (●). The fastest component, τ_1 = 23.4 ± 3.4 ms at +50 mV (n = 6) could be seen only at temperatures above 32°C and was no longer observable when the temperature was subsequently decreased (data not shown). The three time constants appeared voltage independent up to 45°C (Fig. 7 *C*), and any temperature dependence was limited (less than twofold change between 22°C and 36°C; Fig. 7 *C*). However, the amount of inactivation increased significantly with temperature (Fig. 7 *D*). Also, the amplitude of the slowest observable component did not change significantly at higher temperatures (Fig. 7 *D*).

Multiple components of the recovery from inactivation

To examine further the relationship between open and inactivated states we examined the recovery from inactivation

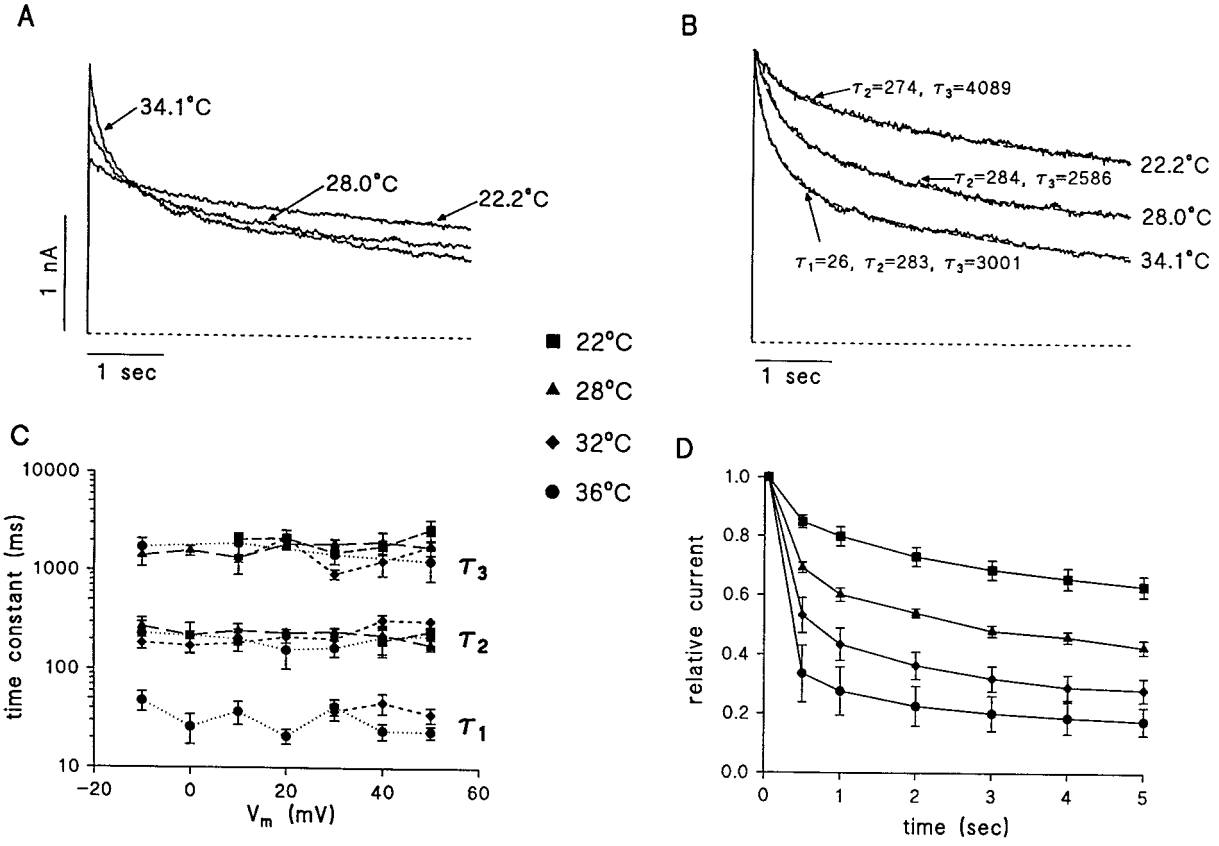

FIGURE 7 Temperature dependence of hKv1.5 inactivation. (*A*) Current traces elicited by 5-s depolarizations to +50 mV at 22.2°C, 28°C, and 34.1°C. (*B*) Currents from *A* normalized to the peak current. The dashed lines are multiexponential fits (22.2°C: τ_2 = 274, τ_3 = 3450 ms; 28.0°C: τ_2 = 284, τ_3 = 2590 ms; 34.1°C: τ_1 = 26, τ_2 = 283, τ_3 = 3001 ms). (*C*) Voltage and temperature dependence of inactivation time constants (■, 22°C; ▲, 28°C; ◆, 32°C; ●, 36°C). (*D*) Temperature dependence of relative inactivation, current normalized to peak value (symbols are the same as in *C*). Data represent at least six experiments (mean ± SEM). The time constants of inactivation appear both temperature and voltage independent, but the amount of inactivation is highly temperature dependent.

using a twin-pulse protocol: an initial 2- or 20-s depolarization, P1 (+50 mV), followed by recovery interval of variable duration (10–2560 ms) at membrane potentials between −120 and −60 mV, and then a 500-ms depolarization, P2 (+50 mV) (see inset of Fig. 8 *A*). To account for cell-to-cell variability in the degree of inactivation, we normalized the fractional recovery from inactivation as follows (Levy and Deutsch, 1996):

$$f_{\text{recov}} = \frac{I_{\text{p1}} - I_{\text{plateau}}}{I_{\text{p2}} - I_{\text{plateau}}},$$

where I_{p1} represents the peak current during pulse P1, I_{p2} represents the peak current during pulse P2, and I_{plateau} represents the level of current at the end of pulse P1. Fig. 8, *B* and *C*, show the recovery from inactivation after a 2-s depolarization in 145 and 4 mM external K^+, respectively. Two components of recovery from inactivation were observed in both high and low external K^+ conditions (Fig. 8, *E* and *F*). No obvious voltage dependence of the faster components was observed; only the slower components displayed a weak voltage dependence. The comparison of recovery from inactivation after 2- and 20-s depolarizations (Fig. 8 *D*) revealed a slowing of the time constants (Fig. 8, *F* and *G*).

DISCUSSION

The major findings of this study were 1) channel opening displayed a primary fast component and a secondary slow component, 2) the rate of channel closure was dependent on the length of the preceding depolarization, and 3) induction of and recovery from inactivation proceeded with at least two exponential components. These results suggest the existence of both multiple open and inactivated states.

A second component of activation occurs after initial activation

A second component of hKv1.5 activation remained after much of the primary component had been eliminated by 5-s depolarizations to −20 and −10 mV. The time constant of each component was independent of prepulse voltage. If the second component of activation were due to a hesitant state in the activation pathway, prepulses to potentials near the

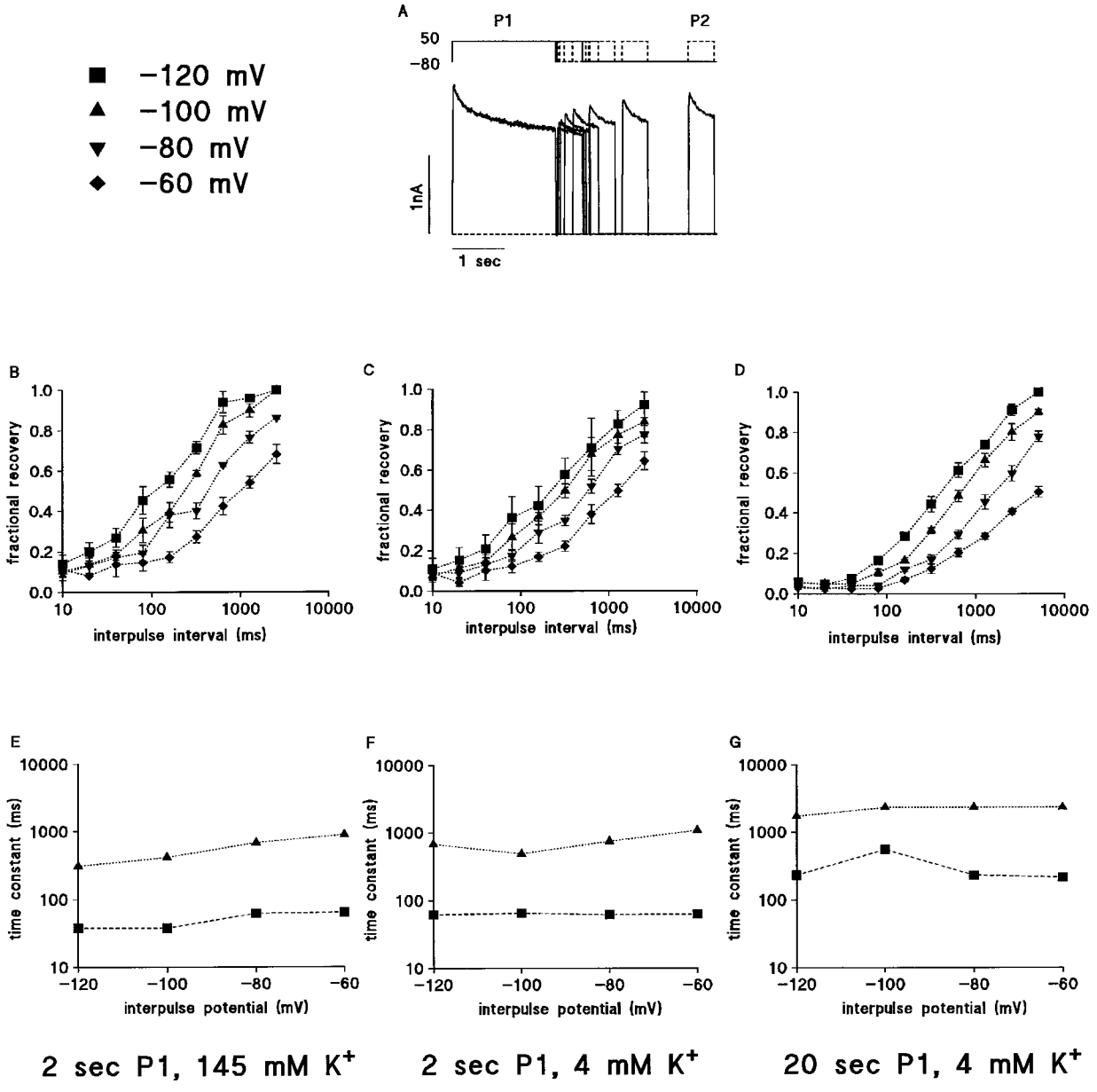

FIGURE 8 Voltage dependence of the recovery from inactivation in 4 and 145 mM external K^+. (*A*) hKv1.5 currents elicited by a 2-s pulse to +50 mV, P1, followed by a variable duration interpulse to −80 mV and then a 500-ms pulse to +50 mV, P2 (inset depicts pulse protocol) in 4 mM external K^+. (*B*) Fractional recovery from inactivation accumulated during a 2-s conditioning pulse in 145 mM external K^+ (■, −120-mV recovery potential; ▲, −100-mV recovery potential; ▼, −80-mV recovery potential; ♦, −60-mV recovery potential). (*C*) Fractional recovery from inactivation accumulated during a 2-s conditioning pulse in 4 mM external K^+ (symbols are the same as in *B*). (*D*) Fractional recovery from inactivation accumulated during a 20-s conditioning pulse in 4 mM external K^+ (symbols are the same as in *B*). (*E*) Components of the recovery from inactivation after a 2-s conditioning pulse in 145 mM external K^+. (*F*) Components of the recovery from inactivation after a 2-s conditioning pulse in 4 mM external K^+. (*G*) Components of the recovery from inactivation after a 20-s conditioning pulse in 4 mM external K^+. Complete recovery from inactivation is quicker in 145 mM external K^+ than in 4 mM external K^+.

threshold of activation should have reduced the occupancy of this hesitant state. However, our results show that the second component of activation is not significantly altered by long prepulses above the threshold of channel activation, suggesting that the second component of activation was due to a process that occurred after initial activation; i.e., it reflects a redistribution of channels between conducting states. Although these data could reflect parallel activation of two populations of channels, our other observations make this unlikely (see below).

A second open state is revealed during deactivation

Tail currents recorded in both low and high external K^+ decayed with a biexponential time course. An interesting

observation was that the time course of tail current decay depended on the duration of the activating pulse. The fastest exponential component of tail current decay ($\tau \approx 6.6$ ms at -80 mV) was observable only after a 5-ms depolarization. The slowing of the tail current decay could be explained by the existence of a nonconducting state that recovered through the open state, as is the case with an open channel blocker (Armstrong, 1969, 1971; Furukawa et al., 1989; Snyders et al., 1992; Zagotta et al., 1994b; Valenzuela et al., 1995). To examine this possibility we considered the following scheme: $C \rightleftharpoons O \rightleftharpoons I$, where channels recovering from an inactivated state through the open state contribute to the observed tail currents.

First we examined the case in which inactivation and recovery from inactivation are slower than deactivation, the probable case for tail currents measured at strong hyperpolarizations. To simulate this we changed the initial conditions varying the percentage of channels starting in the inactivated state. In this case, the above scheme could be simplified to $C \leftarrow O \leftarrow I$ because channels entering the open state would be much more likely to close than to inactivate again. In all simulations, the rate of recovery from inactivation and the rate of channel closure (80/s) were chosen to match the fast deactivation time constant at strong hyperpolarizations. These simulations show that even with a fast recovery from inactivation (40/s), 50% of the channels must initially be inactivated to double the time constant of a monoexponential fit (Fig. 9 *A*). To further slow the simulated deactivation time course we needed to decrease the rate of recovery from inactivation. When the latter was decreased sufficiently (10/s), a second exponential component was detectable, but in this case the first exponential component was not significantly altered by increasing the number of channels initially in the inactivated state.

The results of this simplified model are more generally true if many inactivated states exist as long as the recovery

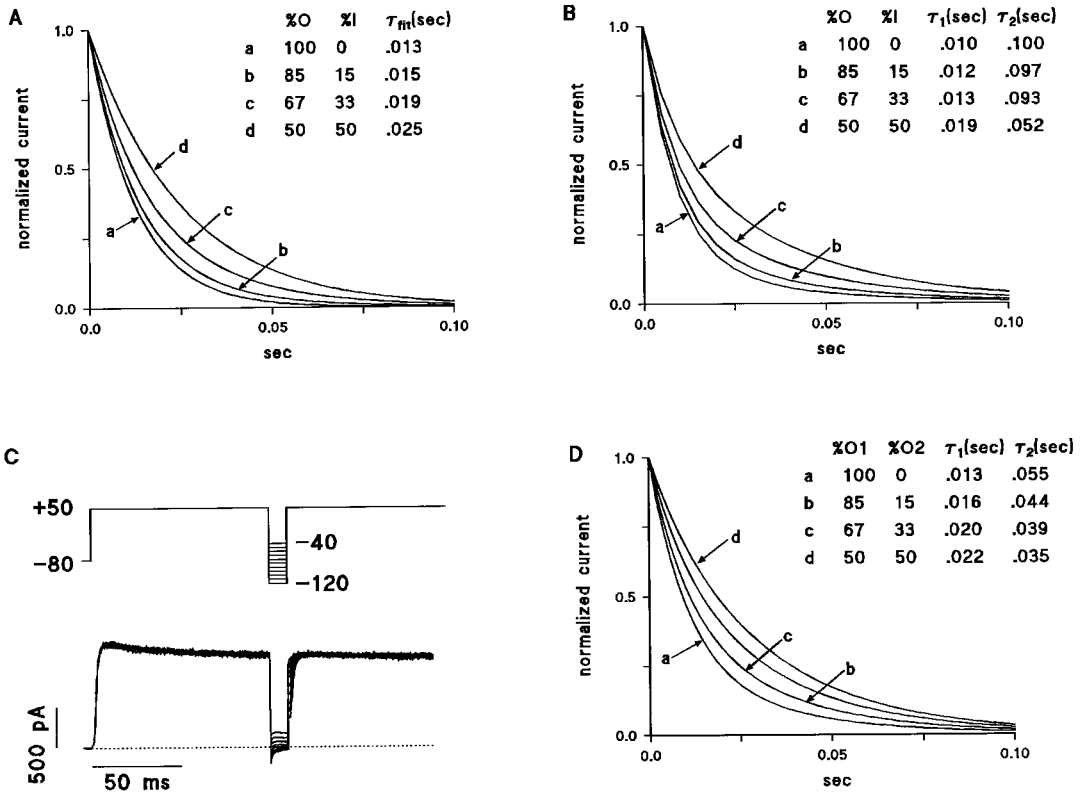

FIGURE 9 Interaction between recovery from inactivation and deactivation. In each simulation, the total amplitude is normalized to unity. (*A*) Simulated tail currents based on three-state model ($C \leftarrow O \leftarrow I$) in which rate constants for the forward transitions are assumed to be much smaller than those for the reverse transitions (see text). A twofold slowing of observed tail currents requires that 50% of the channels initially be in the inactivated state. (*B*) Simulated tail currents for a four-state model ($C \rightleftharpoons C \rightleftharpoons O \rightleftharpoons I$). Again, for a twofold slowing of the tails, 50% of the channels must initially be in the inactivated state. (*C*) Triple-pulse protocol. A triple-pulse protocol (depicted above) was used to test for a fast (hidden) component of inactivation or recovery from inactivation. No excess current was observed after a 10-ms intermediate step to potentials between -40 and -120 mV. Note that the slow component of activation is always observable during the second step to $+50$ mV. This experiment is representative of the results for intermediate step durations between 2 and 40 ms. (*D*) Simulations for a model with multiple open states ($C \rightleftharpoons O \rightleftharpoons O$). Note the similarity in the time course for tail current decay between the models simulated in *A*, *B*, and *D*. The difference is that the model simulated in *D* does not require 50% of the channels to be inactivated to slow the tail current time course twofold. With 50% of the channels initially in the second open state, the first exponential component of the tail current decay is slowed almost twofold. Even with only 33% of the channels allocated to the second open state, a significant slowing is observed. In either case, this is achieved without a decrease in total amplitude.

from inactivation is slow compared with deactivation. It might be argued that more complex schemes with nonzero forward rates could produce the observed slowing of tail currents. This was examined with the following model:

$$C \underset{k_{12}}{\overset{k_{21}}{\rightleftharpoons}} C \underset{k_{23}}{\overset{k_{32}}{\rightleftharpoons}} O \underset{k_{34}}{\overset{k_{43}}{\rightleftharpoons}} I,$$

where k_{21} = 2.25/s, k_{32} = 1.125/s, k_{34} = 20/s, k_{12} = 20/s, k_{23} = 80/s, and k_{34} = 40/s (Fig. 9 *B*). Even with a relatively fast recovery from inactivation, >50% of the channels must be inactivated to double the time constant of the fast exponential component. In this simulation, the second exponential component actually became faster as the initial percentage of inactivated channels was increased because of the relatively fast recovery from inactivation. This did not occur when k_{34} was decreased from 40/s to 10/s; however, this reduced the slowing of the fast component of deactivation. The experimental data show that reduction of tail current amplitudes (~15% after 50- and 500-ms pulses) was consistent with the reduction of current due to the small amount of slow inactivation (~14%); this small amount of inactivation could not account for the slowing of the tail current decay. Thus, these simulations support the qualitative argument that the small increase in inactivation does not properly explain the substantial slowing of both exponential components in the deactivating tail currents.

It is possible that recovery from a rapid (hidden) inactivation component could contribute to the slowing of the tail currents. This type of inactivation has been previously described for the HERG channel (Smith et al., 1996; Snyders and Chaudhary, 1996; Spector et al., 1996). This is analogous to the effects of tetraethylammonium block of K^+ channels (Armstrong, 1969, 1971), the effects of quaternary ammonium derivatives on *Shaker* (Choi et al., 1993), and the effects of quinidine block of hKv1.5 (Snyders et al., 1992). To test this possibility, we again used the triple-pulse protocol (inset of Fig. 9 *C*). We did not observe an increase in peak current in any of these experiments. A voltage-independent form of fast inactivation, similar to the flicker state described by Hoshi et al. (1994) could also account for the slowing of the tails. The rates into and out of this flicker state would have to be significantly faster than other transitions near the open state. However, this is not consistent with the data showing a twofold slowing of the fast exponential component of tail current decay after 50- and 500-ms activating pulses. Indeed, if the transitions into the flicker state were fast enough not to be observed during depolarization, then occupancy in this state would have reached a quasi-equilibrium before 50 ms.

Simulations with a second open state

As the above simulations with a single open state and with experimentally required constraints on the inactivated state transitions fail to account for the observed deactivation kinetics, let us now consider simulations based on multiple open states. Fig. 9 *D* shows simulations based on the following scheme:

$$C \underset{k_{12}}{\overset{k_{21}}{\rightleftharpoons}} O \underset{k_{23}}{\overset{k_{32}}{\rightleftharpoons}} O,$$

where k_{21} = 1.13/s, k_{32} = 1/s, k_{12} = 80/s, and k_{23} = 30/s and both open states have the same conductance. In this model, we have not considered the possibility that both open states reflect parallel pathways between the closed state(s) and the inactivated state(s) because the prepulse dependence of the contribution of the fast and slow components of activation (Fig. 3) indicates that the slow component of activation occurs after the fast component. Furthermore, such parallel activation should not lead to a progressive slowing of tail currents (a relative change in amplitude of each component with unchanged time constants would be expected). We have also neglected inactivation to demonstrate that a multiple open state model can account for the slowing of tail current decay without requiring the assumption that recovery from inactivation occurs through the open states.

We found that when 33–50% of the channels are initially in the second open state, the time constant of the fast exponential component was almost twofold slower than when all of the channels were in the first open state. Obviously, this happens without a change in total amplitude in this model (in contrast to simulations in Fig. 9, *A* and *B*). Thus, this model illustrates that the slowing of the tail current time course can easily be reproduced by transitions between multiple open states rather than contributions from inactivated states recovering through a single open state.

Multiple inactivated states preceded by a second open state

At temperatures above 32°C three distinct components of inactivation were observed during depolarization. The components of inactivation displayed essentially voltage-independent time constants with limited temperature dependence; however, the relative amplitudes of these components were highly voltage and temperature dependent.

These observations imply that a transition preceding inactivation limits the number of channels available for inactivation and that this process is both voltage and temperature dependent. This can be demonstrated with a three-state model ($O \rightleftharpoons I \rightleftharpoons I$). If the rate constants are to satisfy 1) the voltage and temperature independence of the time constants and 2) the voltage and temperature dependence of their relative amplitudes, then at least one of the rate constants must be negative, which is nonsensical (see Appendix). Therefore, the data suggest that a transition before the $O \rightleftharpoons I$ transition limits the number of channels available to enter the inactivated states. Moreover, this rate-limiting transition must be into an open state; indeed, if that transition were into a closed state, then it would be observable as

a voltage- and temperature-dependent inactivation time constant. It is important to note that these data do not imply that inactivation is strictly temperature independent; they imply only that a voltage- and temperature-dependent transition before inactivation limits the number of channels available to inactivate.

The limited voltage dependence of the kinetics of C-type inactivation is consistent with previous reports for the Kv1.5 channel (Snyders et al., 1993), *Shaker* channels lacking N-type inactivation (Hoshi et al., 1994), and native channels in T lymphocytes (Lee and Deutsch, 1990). In a recent analysis of the temperature dependence of inactivation kinetics of *Shaker* mutants, two components were reported for induction of C-type inactivation up to 28°C (Meyer and Heinemann, 1997), which is consistent with our observations; only above 32°C did we observe three components.

Recovery from inactivation occurs through the open states

Although the slowing of the fast exponential component of tail current decay cannot be explained by recovery from C-type inactivation through the open states, several results suggest that recovery from inactivation occurred through the open state. First, the slower time constants of tail current decay were similar to those of the recovery from inactivation. Second, both the tail current decay and the recovery from inactivation were accelerated in high external K^+. Third, when comparing deactivating currents after 500-and 5000-ms prepulses (Fig. 5), tail current crossover always occurred. The reduction in initial current is consistent with the amount of inactivation whereas the marked slowing of tail currents after 5- and 20-s prepulses is consistent with either very long-lived open states or recovery from inactivation through the open states.

Possible contributions from endogenous currents or subunits

We have previously shown that *Ltk*$^-$ cells express an endogenous β-subunit (Kvβ2.1) (Uebele et al., 1996). Together with the possibility of endogenous currents, this leads to the possibility that the data we have presented may reflect multiple populations of K^+ channels rather than multiple open states of the hKv1.5 channel. However, we do not believe this to be the case for several reasons. First, Fig. 1 shows that the largest endogenous currents we observed had little or no time varying component during depolarization or subsequent repolarization (both at 23°C and 33°C). Second, the putative contamination by an endogenous current should be more marked in cells expressing small hKv1.5 currents. However, the second component of activation always represented ≈30% of the activation time course regardless of the total amplitude of the measured currents (300 pA to 3 nA). Third, the slowing of tail current time constants with extended prepulses was a consistent finding regardless of the amplitude of the tail currents (i.e., the relative amplitudes were similar). Furthermore, we do not believe that the endogenous β-subunit creates the multiple open states because we have observed similar results in HEK293 cells (two components of activation, slowing of tail currents with extended prepulses, temperature-independent inactivation time constants; data not shown). These cells lack the endogenous Kvβ2.1 subunit found in *Ltk*$^-$ cells (Uebele et al., 1996). Finally, as argued above, if the data reflect parallel activation of two populations of channels, we should observe components of deactivation with amplitudes reflecting the amount of activation of each population but without progressive change in time constants.

CONCLUSION

The data presented here strongly suggest that the hKv1.5 channel has multiple open and inactivated states and that slow entry into the later open states limits the amount of inactivation observable at room temperature. A simple conceptual model can account for the data we have presented:

$$C \rightleftharpoons C \rightleftharpoons \ldots \rightleftharpoons C \rightleftharpoons O \rightleftharpoons O \rightleftharpoons I \rightleftharpoons I \rightleftharpoons I$$

According to this model, the delay in activation is due to multiple closed states before the activated state, the second component of activation is due to an equilibration between the multiple open states, the tail current time course depends on the duration of the activating pulse, and the amount of inactivation increases as temperature increases due to a temperature-dependent increase in the transition rates between open states.

APPENDIX

To address the possibility that the rate constants of a system can be changed in a manner that holds the apparent time constants of the system constant while substantially modifying the relative amplitudes, we have examined a simple three-state system. We show that to meet the above criteria at least one rate constant must be negative. To start, consider this simple, three-state model, which exhibits multiexponential behavior:

$$O \underset{k_{12}}{\overset{k_{21}}{\rightleftharpoons}} I_1 \underset{k_{23}}{\overset{k_{32}}{\rightleftharpoons}} I_2$$

The analytical solution of this system has the following form:

$$O(t) = A + Be^{-\lambda_1 t} + Ce^{-\lambda_2 t},$$

where

$$\lambda_{1,2} = 0.5\Big\{k_{12} + k_{21} + k_{23} + k_{32} \pm \sqrt{k_{12}^2 + k_{21}^2 + k_{23}^2 + k_{32}^2 + 2(k_{12}k_{21} + k_{12}k_{32} + k_{23}k_{32} - k_{12}k_{23} - k_{21}k_{23} - k_{21}k_{32})}\Big\},$$

and A, B, and C are functions of both the rate constants, k_{ij}, and the initial conditions. In principle, the rate constants are functions of both voltage and

temperature. We have shown that the inactivation time constants are voltage and temperature independent but that their relative amplitudes are substantially temperature dependent. Thus, the temperature dependence of the inactivation amplitudes must be due to a rate-limiting step occurring before the O $\rightleftharpoons$ I transition. This point can be demonstrated by examining the solution to the simple model given above. If the apparent time constants of inactivation are to remain constant, the following relations must hold:

$$k_{12} + k_{21} + k_{23} + k_{32} = \lambda_1 + \lambda_2 \quad \text{(A1)}$$

$$k_{12}k_{23} + k_{21}k_{23} + k_{21}k_{32} = \lambda_1\lambda_2, \quad \text{(A2)}$$

where λ_1 and λ_2 are the eigenvalues of the system. The eigenvalues of the system must remain constant for the observed time constants to remain constant. Assuming that all of the channels are initially open, $O_{t0} = 1$, the amplitude terms are given by

$$B = 1 - O_\infty - C \quad \text{(A3)}$$

$$C = \frac{k_{12} + k_{23} + k_{32} - \lambda_2 - \lambda_1 O_\infty}{\lambda_1 - \lambda_2}, \quad \text{(A4)}$$

where O_∞ is the steady-state open probability. The observation that the amplitude term of one component of inactivation appears temperature independent whereas the other amplitude term appears highly temperature dependent means that we can consider one amplitude term, e.g., C, constant. This gives the following relation:

$$k_{21} = \frac{-k_{12}k_{23}}{\lambda_2} + C(\lambda_1 - \lambda_2) - \lambda_1 \quad \text{(A5)}$$

At temperatures below 17°C and infrequently at room temperature (<15% of experiments), inactivation follows a monoexponential time course (data not shown). Therefore, under these conditions, we can consider *B* equal to zero, which gives the following relation:

$$k_{12} = \frac{(1 - C)\lambda_1\lambda_2}{k_{23}} \quad \text{(A6)}$$

Solving Eqs. A1, A2, A5, and A6 reveals that for the above relations to be true k_{21} must be negative. Thus, it is not possible to adjust the rate constants to describe the range of relative amplitudes observed without modifying the apparent time constants.

This work was supported by National Institutes of Health Grants HL47599, HL46681, HL07411, and GM08452.

REFERENCES

Armstrong, C. M. 1969. Inactivation of the potassium conductance and related phenomena caused by quaternary ammonium ion injection in squid axons. *J. Gen. Physiol.* 54:553–575.

Armstrong, C. M. 1971. Interaction of tetraethylammonium ion derivatives with the potassium channels of giant axons. *J. Gen. Physiol.* 58: 413–437.

Barry, P. H., and K. W. Lynch. 1991. Liquid junction potentials and small cell effects in patch-clamp analysis. *J. Membr. Biol.* 121:101–117.

Bezanilla, F., E. Perozo, and E. Stefani. 1994. Gating of *Shaker* K^+ channels. II. The components of gating currents and a model of channel activation. *Biophys. J.* 66:1011–1021.

Choi, K. L., C. Mossman, J. Aube, and G. Yellen. 1993. The internal quaternary ammonium receptor site of *Shaker* potassium channels. *Neuron*. 10:533–541.

Cole, K. S., and J. W. Moore. 1960. Potassium ion current in the squid giant axon: dynamic characteristic. *Biophys. J.* 1:1–14.

Correa, A. M., and F. Bezanilla. 1994. Gating of the squid sodium channel at positive potentials. I. macroscopic ionic and gating currents. *Biophys. J.* 66:1853–1863.

Deal, K. K., S. K. England, and M. M. Tamkun. 1996. Molecular physiology of cardiac potassium channels. *Physiol. Rev.* 76:49–76.

Feng, J., B. Wible, G. R. Li, Z. G. Wang, and S. Nattel. 1997. Antisense oligodeoxynucleotides directed against Kv1.5 mRNA specifically inhibit ultrarapid delayed rectifier K^+ current in cultured adult human atrial myocytes. *Circ. Res.* 80:572–579.

Furukawa, T., Y. Tsujimura, K. Kitamura, H. Tanaka, and Y. Habuchi. 1989. Time- and voltage-dependent block of the delayed K^+ current by quinidine in rabbit sinoatrial and atrioventricular nodes. *J. Pharmacol. Exp. Ther.* 251:756–763.

Hoshi, T., W. N. Zagotta, and R. W. Aldrich. 1991. Two types of inactivation in Shaker K^+ channels: effects of alterations in the carboxy-terminal region. *Neuron*. 7:547–556.

Hoshi, T., W. N. Zagotta, and R. W. Aldrich. 1994. *Shaker* potassium channel gating. I. Transitions near the open state. *J. Gen. Physiol.* 103:249–278.

Lee, S. C., and C. Deutsch. 1990. Temperature dependence of K^+-channel properties in human T lymphocytes. *Biophys. J.* 57:49–62.

Levy, D. I., and C. Deutsch. 1996. Recovery from C-type inactivation is modulated by extracellular potassium. *Biophys. J.* 70:798–805.

Malayev, A. A., D. J. Nelson, and L. H. Philipson. 1995. Mechanism of clofilium block of the human Kv1.5 delayed rectifier potassium channel. *Mol. Pharmacol.* 47:198–205.

Mays, D. J., J. M. Foose, L. H. Philipson, and M. M. Tamkun. 1995. Localization of the Kv1.5 K^+ channel protein in explanted cardiac tissue. *J. Clin. Invest.* 96:282–292.

Meyer, R., and S. H. Heinemann. 1997. Temperature and pressure dependence of *Shaker* K^+ channel N- and C-type inactivation. *Eur. Biophys. J.* 26:433–445.

Neher, E. 1992. Correction for liquid junction potentials in patch clamp experiments. *Methods Enzymol.* 207:123–131.

Philipson, L. H., R. E. Hice, K. Schaeffer, J. LaMendola, G. I. Bell, D. J. Nelson, and D. F. Steiner. 1991. Sequence and functional expression in *Xenopus* oocytes of a human insulinoma and islet potassium channel. *Proc. Natl. Acad. Sci. U.S.A.* 88:53–57.

Smith, P. L., T. Baukrowitz, and G. Yellen. 1996. The inward rectification mechanism of the HERG potassium channel. *Nature*. 379:833–836.

Snyders, D. J., and A. C. Chaudhary. 1996. High affinity open-channel block by dofetilide of *HERG*, expressed in a human cell line. *Mol. Pharmacol.* 49:949–955.

Snyders, D. J., K. M. Knoth, S. L. Roberds, and M. M. Tamkun. 1992. Time-, voltage-, and state-dependent block by quinidine of a cloned human cardiac potassium channel. *Mol. Pharmacol.* 41:322–330.

Snyders, D. J., M. M. Tamkun, and P. B. Bennett. 1993. A rapidly activating and slowly inactivating potassium channel cloned from human heart: functional analysis after stable mammalian cell culture expression. *J. Gen. Physiol.* 101:513–543.

Snyders, D. J., and S. W. Yeola. 1995. Determinants of antiarrhythmic drug action: electrostatic and hydrophobic components of block of the human cardiac hKv1.5 channel. *Circ. Res.* 77:575–583.

Spector, P. S., M. E. Curran, A. Zou, M. T. Keating, and M. C. Sanguinetti. 1996. Fast inactivation causes rectification of the I_{Kr} channel. *J. Gen. Physiol.* 107:611–619.

Stefani, E., L. Toro, E. Perozo, and F. Bezanilla. 1994. Gating of *Shaker* K^+ channels: I. Ionic and gating currents. *Biophys. J.* 66:996–1010.

Tamkun, M. M., K. M. Knoth, J. A. Walbridge, H. Kroemer, D. M. Roden, and D. M. Glover. 1991. Molecular cloning and characterization of two voltage-gated K^+ channel cDNAs from human ventricle. *FASEB J.* 5:331–337.

Uebele, V. N., S. K. England, A. C. Chaudhary, M. M. Tamkun, and D. J. Snyders. 1996. Functional differences in Kv1.5 currents expressed in

mammalian cell lines are due to the presence of endogenous Kvβ2.1 subunits. *J. Biol. Chem.* 271:2406–2412.

Valenzuela, C., E. Delpon, M. M. Tamkun, J. Tamargo, and D. J. Snyders. 1995. Stereoselective block of a human cardiac potassium channel (Kv1.5) by bupivacaine enantiomers. *Biophys. J.* 69:418–427.

Wang, Z., B. Fermini, and S. Nattel. 1993. Sustained depolarization-induced outward current in human atrial myocytes: evidence for a novel delayed rectifier K^+ current similar to Kv1.5 cloned channel currents. *Circ. Res.* 73:1061–1076.

Zagotta, W. N., and R. W. Aldrich. 1990. Voltage-dependent gating of Shaker A-type potassium channels in *Drosophila* muscle. *J. Gen. Physiol.* 95:29–60.

Zagotta, W. N., T. Hoshi, and R. W. Aldrich. 1994a. *Shaker* potassium channel gating. III. Evaluation of kinetic models for activation. *J. Gen. Physiol.* 103:321–362.

Zagotta, W. N., T. Hoshi, J. Dittman, and R. W. Aldrich. 1994b. *Shaker* potassium channel gating. II. Transitions in the activation pathway. *J. Gen. Physiol.* 103:279–319.